Excitation and propagation of surface plasmons on metallic nanowires

Xiaorui Tian[a], Ning Liu[a], Hong Wei[a], Hongxing Xu*[a,b]
[a]Beijing National Laboratory for Condensed Matter Physics and Institute of Physics, Chinese Academy of Sciences, PO Box 603-146, Beijing 100190, China; [b]Division of Solid State Physics/The Nanometer Structure Consortium, Lund University, PO Box 118, Lund, S-22100, Sweden

ABSTRACT

The comprehensive understanding of the excitation and propagation of surface plasmons (SPs) on metallic nanowires (NWs) is essential for potential applications of these materials as nanoscale optical waveguides. Combining theory and different experimental methods, we did intensive study on the excitation and propagation of SP modes in crystal Ag nanowires. We found the excitation of NW SP modes is strongly affected by the excitation configuration. When an optically "thick" NW is radiated at the end of the NW, several SP modes could be excited simultaneously with appropriate incident polarization. If the NW is in the medium of uniform refractive index, the coherent superposition of these SP modes generates chiral SPs in single NW, and the handedness of the chiral SPs can be controlled by the input polarization angle. When we use a near field scanning optical fiber tip to excite the SPs on metallic nanowires from the middle of the NW, we also found multiple SP modes in the NWs can be excited through polarization selective near field interaction. The excitation mechanism of the tip-induced SP propagation is quite different from the previous wire-end-launching scheme. We found the input coupling efficiency is modulated by Fabry-Pérot interferences in the near field coupling case.

Keywords: surface plasmons, chiral, handedness, near-field scanning optical microscopy, Fabry-Pérot interferences

1. INTRODUCTION

Surface plasmons (SPs), collective oscillations of free electron gas at the interface of metal and dielectric, offer a platform for manipulating light at the nanometer scale and enable a wide range of applications such as surface-enhanced Raman scattering (SERS),[1-4] sensing,[5-8] optical forces,[9-11] subwavelength circuitry and nanolasing,[12, 13] and so on. SPs can be localized into a deep subwavelength region ('hot site') that typically resides in coupled metal nanostructures, such as nanoparticle dimer,[3, 14, 15] nanohole-nanoparticle,[16] nanowire-nanoparticle,[17, 18] and nanoparticle-metal film.[19] The huge electromagnetic field enhancement due to the strong coupling of surface plasmons firstly discovered in 1999[3] has become the base not only for single molecule SERS,[3, 4, 14] but also for many emerging phenomena and subfields of plasmonics, including plasmonic antenna,[20] interplay between SERS and surface enhanced fluorescence,[21, 22] plasmon-enhanced optical force,[9, 11] plasmon hybrization,[23] and quantum plasmonics.[24-27]

SPs can propagate along the metal-dielectric interface over a certain distance. Many architectures have been proposed for guiding SPs beyond the diffraction limit. Among these, metallic nanowires (NWs) have attracted significant interest in the past decade.[28, 29] Intensive studies about SP propagation on the metallic nanowires have been performed recently, including remote-excitation SERS and quantum dot fluorescence,[18, 30] emission directionality at the NW terminals,[31, 32] correlation between incident and emission polarization,[33] the effect of substrates and bending on the propagating loss of SPs,[34, 35] and the excitation and propagation of multiple SP modes on metallic NWs.[36, 37] Besides, some NWs-based plasmonic devices have been realized, such as routers, modulators, and all-optical Boolean logic gates that can perform simple computational operations.[38-41] These studies may have significant effects on the future integrated plasmonic circuitry, see e.g. our recent review.[42]

In this paper, we summarize our recent studies on SP modes and propagation of these modes in Ag nanowires.[36, 37] We found the excitation of the SP modes on metallic NWs is strongly dependent on the excitation configuration. In the commonly used wire-end-launching configuration, several plasmon modes can be excited simultaneously by the incident light with an appropriate polarization. The coherent superposition of the three lowest specific nanowire waveguide

Plasmonics: Metallic Nanostructures and Their Optical Properties X, edited by Mark I. Stockman,
Proc. of SPIE Vol. 8457, 84571N · © 2012 SPIE · CCC code: 0277-786/12/$18 · doi: 10.1117/12.931298

modes generates chiral SPs on metallic NWs. Using quantum dots as local-field reporters, we experimentally observed chiral SPs on individual nanowires. The handedness, spatial extent and the helical periods of the chiral SPs depend on the input polarization angle, the nanowire diameter and the dielectric environment. By using a scanning optical fiber tip, we can excite the SP modes on metallic NWs from the middle of the NWs. The excitation mechanism of this excitation configuration is quite different from the above wire-end-launching scheme. Our study shows that multiple SP modes in Ag NWs can be triggered through polarization selective near field interaction.

2. WIRE-END-LAUNCHED CHIRAL SURFACE PLASMONS ON METALLIC NANOWIRES

Plasmonic circuitry is considered promising for miniaturizing and integrating the next generation of optical nano-devices. Due to their single crystal structure, smooth surface and well-defined geometry, chemically synthesized metallic NWs have attracted much attention as subwavelength SP waveguides. Comprehensive understanding of the excitation of SP modes in cylindrical NWs is of pivotal importance for the potential applications. We theoretically show that chiral SPs can be generated on metallic nanowires by exciting a superposition of nanowire SP modes. The handedness of the chiral SPs can be controlled by simply changing the incident light polarization.

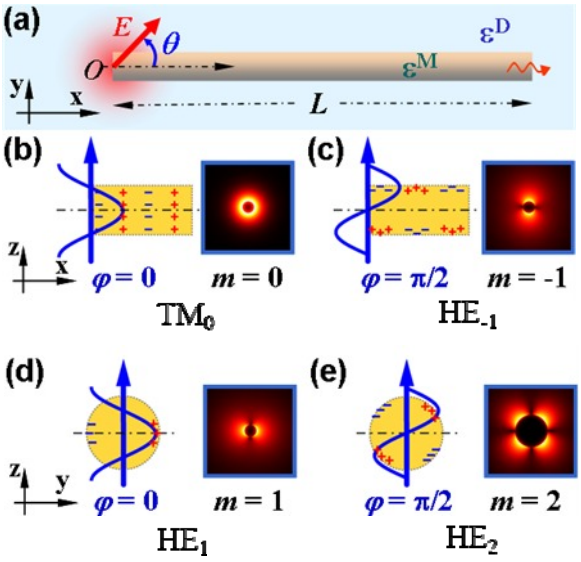

Figure 1. (a) Calculation model. (b-e) SP modes (named TM_0, HE_{-1}, HE_1 and HE_2, respectively) excited by the incident light with appropriate polarization illuminating on the terminus of the NW. The radius R of the simulated Ag nanowire is 60 nm in (b-d) and 250 nm in (e). The permittivity of the embedding medium is 2.25 and the incident wavelength is 632.8 nm in vacuum. (reproduced from ref.36)

Figure 1(a) gives the calculation model in the finite element method we used. The NW is embedded in a homogeneous environment, which is essential for the observation of the chiral SPs. In experiments, we realized such a system by depositing Ag NWs on glass slides and coating them with index-matching oil. A paraxial Gaussian beam excites the SPs at one end of the metallic NW. Figures 1(b) – 1(e) show the several lowest plasmon modes existing in a optically "thick" NWs. These modes can be selectively excited by tuning the incident polarization. When the incident excitation is neither parallel to, nor perpendicular to the axis of the NW, m = 0, 1, -1 modes (we just consider the three lowest modes) can be simultaneously excited. Due to the retardation effect, the phases are different for these modes. HE_{-1} mode always has a phase difference $\Delta\Phi = \pm\pi/2$ from that of HE_1 mode. Therefore, when the SPs propagates along the NW, the coherent interference of HE_{-1} mode and HE_1 mode with equal amplitude ($\theta = 45^{\circ}$) can generate a circularly polarized wave. The circularly polarized SPs then interfere with the TM_0 mode, resulting in a helical wave which propagates along the NW. The helical propagating SPs are clearly reflected by the helical distribution of the surface charge density in Figure 2(a). The rotation of power flow along the NW shown in Figure 2(b) further confirms the helical wave. The handedness of the chiral SPs can be controlled simply by tuning the incident polarization, which determines the phase delay between the

HE_1 and HE_{-1} modes. An advanced phase for the HE_1 mode relative to the HE_{-1} mode results in right-handed SPs, and a delayed phase results in left-handed SPs. Using quantum dot-based fluorescence imaging method, the right- and left-handed chiral SPs are observed experimentally, as shown in Figure 2(c) (ii) and (iii), respectively. The helical field pattern disappears when the polarization is either parallel (iv) or perpendicular (v) to the nanowire, due to the missing of HE_1 or TM_0 mode. It should be noted that the emitted light at the output terminal of the NW can keep the chirality of the SPs, resulting in circularly polarized output light, which makes the NW functioning as a subwavelength quarter wave-plate to convert linearly polarized light to circularly polarized light.

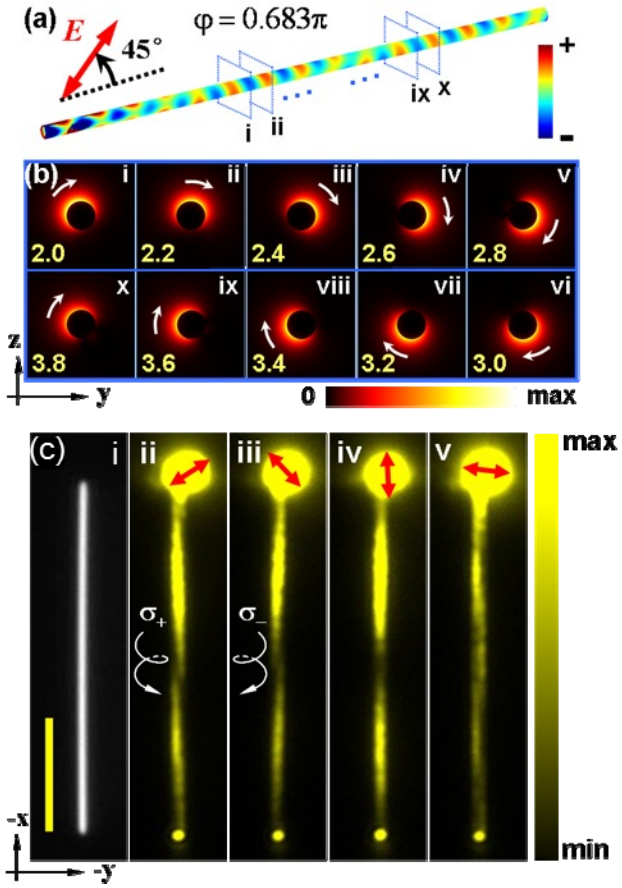

Figure 2. Chiral SPs. (a) Surface charge density plot on a Ag nanowire (R = 60 nm). (b) Time-averaged power flow in the *yz* plane at different positions along the nanowire, where x = 2.0 to 3.8 μm (i-x) in steps of 0.2 μm, indicated by the blue frames in (a). The white arrows highlight the rotation of electromagnetic energy as a function of position along metallic nanowire, showing right-handed chiral SPs. (c) Experimentally observed chiral SPs through quantum dot fluorescence images (ii - v). Optical image of a Ag nanowire was shown in (i). The scale bar is 5 μm. (reproduced from ref.36)

3. SURFACE PLASMONS ON METALLIC NANOWIRES INDUCED BY NEAR FIELD SCANNING OPTICAL FIBER TIP

Most studies on the SP modes and their propagation on metallic NWs are based on wire-end-launching configuration, which means the incident light excites the SPs from the end of the NW. However, the design of plasmonic or hybrid photonic-plasmonic devices needs various configurations of excitation,[39, 40] so the comprehensive understanding of how the light excites the SP modes on metallic NWs from the middle of the NW is very important. Using near field raster scanning technique, we report polarization-dependent study on SP modes of metallic NW excited from the middle of the NW through a near field scanning optical fiber tip, which can be fully controlled and varied with nanometer spatial accuracy.

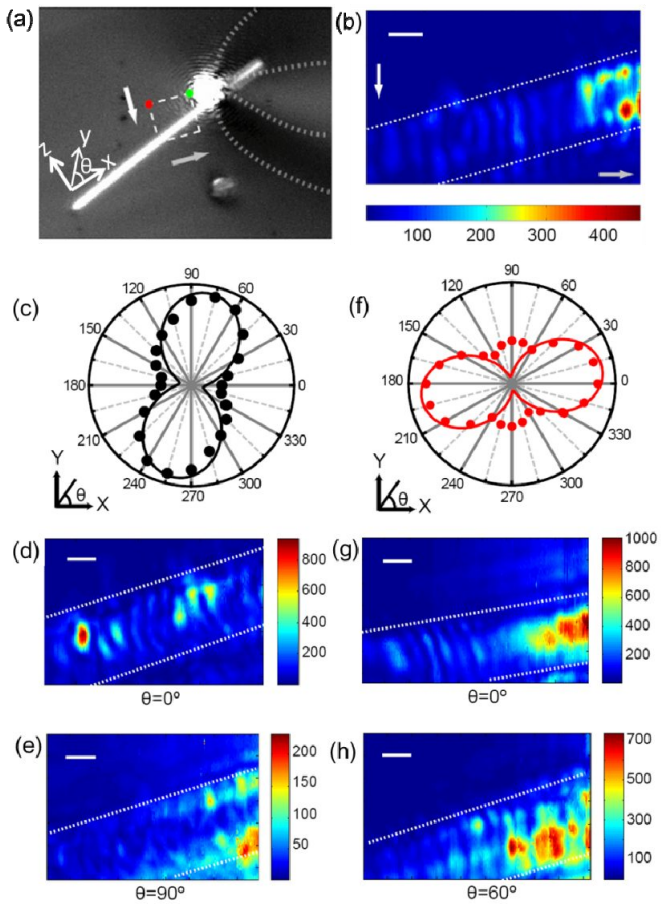

Figure 3. (a) Bright field optical image of an optical fiber tip with input radiation in working distance from a silver nanowire with a diameter of 320 nm and a length of 17 μm. The Ag NW locates in the XY plane. (b) The NSOM image of the area in (a) marked by dashed rectangle. (c)-(h) Experimental study on the effect of the tip position and excitation polarization on the launching of the SP modes in a Ag NW. (c) and (f) are the polarization measurements (solid circles) on two different input radiations. (d) and (e), (g) and (h) are NSOM images for different polarized emission light with input polarization as shown in panel (c) and (f), respectively. The scale bars are 500 nm. (reproduced from ref. 37)

Our experiment is performed on a near-field scanning optical microscopy (NSOM) system. In the experiment, the input laser light (CW 632.8 nm) is coupled into the optical fiber through an objective, and then excites the SP modes from the middle of the NW through near field coupling. The light propagates along the NW in the form of SPs, and couples out at the end the NW and is detected by a CCD camera. The raster scanning is realized by a piezo-driven scanner attached to the fiber tip, which is positioned underneath an upright Olympus optical microscope. During the raster scanning, the intensity of wire-end output is monitored with the CCD camera, and the corresponding tip position is known at all time. Therefore, we can get a 2D false color image as shown in Figure 3(b), which reveals the intensity change of the output light at wire end as a function of tip position when it scans over part of the NW. The tip-launched SP modes are strongly dependent on the tip apex position and the incident polarization. Figures 3(c)-3(h) gives the incident and emission polarization dependent studies when the tip scanned across the NW. It is clearly seen that the intensity patterns change dramatically when different components of the output light are investigated. In the case of Figure 3(c), for the X polarization output, the signal is mostly concentrated in the middle up part of the NW, while for the Y polarization, the strongest intensity is found along the edges of the wire. When the input is polarized near X direction, as in Figure 3(f), if the output component polarized along the X axis is detected, a spatial distribution symmetric along the long axis of the NW is obtained (Figure 3(g)), and if the output is polarized to 60 degrees off the X axis, the strongest signal is acquired with the tip positioned at the bottom half of the NW. These phenomena are closely related with the excitation mechanism of SPs in this tip-induced configuration.

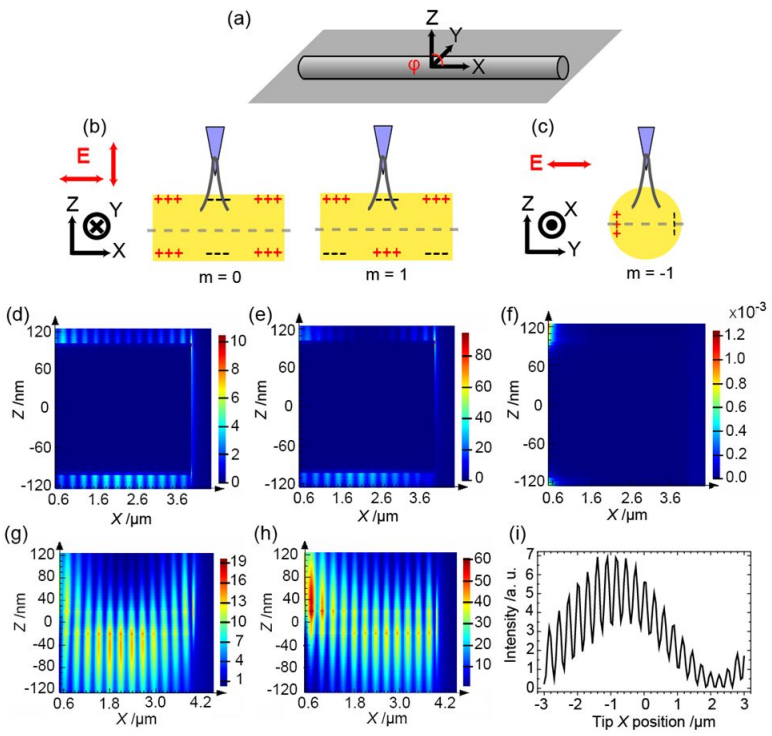

Figure 4. (a) Coordinates of Ag NW in simulation. (b) and (c) Schematics of tip-induced SP modes in Ag NW when the polarization of the input light is along different directions. (d)-(f) Electric field intensity plots of excited SP modes on ZX plane passing the central axis of the NW with the dipole placed at X = 0, Y = 0, Z = 110 nm, polarization along X, Z, and Y directions, respectively. (g)-(h) Intensity plots on ZX plane at Y = -110 nm for Z polarized input radiation with dipole positioned at X = 0 and X = 400 nm, respectively. (i) Output intensity maximum on XY plane at Z = 110 nm, close to the wire end, as a function of input dipole position along X axis, at Y = 0 and Z = 110 nm. (adapted from ref. 37)

Figure 4 shows the excitation mechanism of the tip-induced SP propagation. The input radiation is coupled into the propagating SPs through optical mode overlap. In this excitation configuration, only $m = 0$ and $m = 1$ SP modes are stimulated efficiently (Figure 4(b)), and the $m = -1$ mode is difficult to be excited even for electric field polarized along the Y direction (Figure 4(c)). The $m = 0$ and $m = 1$ SP modes are excited simultaneously for both X and Z polarized input radiation, so a beat pattern can be seen as shown in Figures 4(d) and 4(e). The short period modulation is resulted from the Fabry-Pérot interference, which directly determines the input coupling efficiency at the radiation gap (Figures 4(g) and 4(h)). The long range beat pattern is a result of the constructive or destructive superposition of the two SP modes.

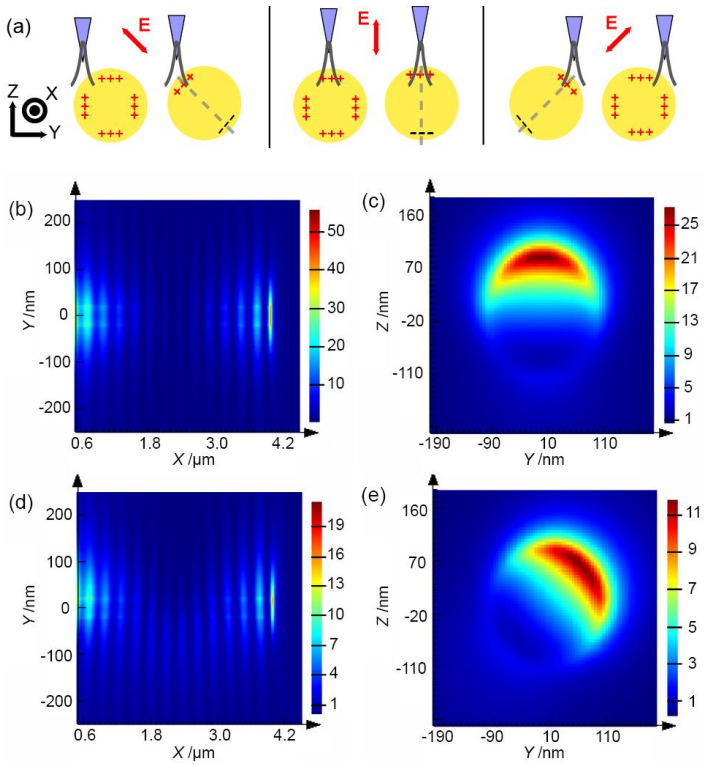

Figure 5. (a) Excitation schematics of the SP modes as the tip moves across the NW with input dipole polarized perpendicular to the central axis of the wire. The red arrows denote the radial polarization direction defined by the tip position. (b) - (d) Intensity plots on different planes when the tip is located at different positions and with different polarizations. (adapted from ref. 37)

Another important conclusion we get from this tip-launched SPs study is that the only component that can be coupled efficiently into SP modes is along the radial direction defined by the tip location, as denoted by the dashed grey line in Figure 5(a). Based on this, when the tip moves toward the edges of the NW, the m = 1 mode rotates around the central axis of the NW, resulting in the long range beat pattern also rotating around the central axis (Figures 5(b)-5(e)). The coupling efficiency decreases when the tip moves to the edges of the NW for Z polarized input, as shown in Figure 5(c) and 5(e), while for X polarized input, it is unchanged. This fact directly influences the patterns obtained in Figures 3(d)-3(h).

SUMMARY

The excitation and propagation of SPs on metallic nanowires have been studied systematically. The excitation of SP modes on NWs is strongly dependent on the excitation configuration and the environmental medium. For a NW in a homogeneous medium, by using wire-end-launching scheme, coherent superposition of the SP modes excited simultaneously makes the NW a good subwavelength quarter wave-plate. For a NW placed on the glass substrate with air as top surroundings, SPs are excited by using the tip-launching configuration, and the output intensity is strongly dependent on the position of the tip and the input polarization.

REFERENCES

[1] M. Moskovits, "Surface-Enhanced Spectroscopy," Rev. Mod. Phys., 57(3), 783-826 (1985).

[2] S. J. Lee, Z. Q. Guan, H. X. Xu *et al.*, "Surface-enhanced Raman spectroscopy and nanogeometry: The plasmonic origin of SERS," J. Phys. Chem. C, 111(49), 17985-17988 (2007).

[3] H. X. Xu, E. J. Bjerneld, M. Käll *et al.*, "Spectroscopy of single hemoglobin molecules by surface enhanced Raman scattering," Phys. Rev. Lett., 83(21), 4357-4360 (1999).
[4] D. K. Lim, K. S. Jeon, H. M. Kim *et al.*, "Nanogap-engineerable Raman-active nanodumbbells for single-molecule detection," Nat. Mater., 9(1), 60-67 (2010).
[5] J. N. Anker, W. P. Hall, O. Lyandres *et al.*, "Biosensing with plasmonic nanosensors," Nat. Mater., 7(6), 442-453 (2008).
[6] H. X. Xu, and M. Käll, "Modeling the optical response of nanoparticle-based surface plasmon resonance sensors," Sensor Actuat. B-Chem., 87(2), 244-249 (2002).
[7] A. J. Haes, L. Chang, W. L. Klein *et al.*, "Detection of a biomarker for Alzheimer's disease from synthetic and clinical samples using a nanoscale optical biosensor," J. Am. Chem. Soc., 127(7), 2264-2271 (2005).
[8] S. P. Zhang, K. Bao, N. J. Halas *et al.*, "Substrate-Induced Fano Resonances of a Plasmonic: Nanocube: A Route to Increased-Sensitivity Localized Surface Plasmon Resonance Sensors Revealed," Nano Lett, 11(4), 1657-1663 (2011).
[9] H. X. Xu, and M. Käll, "Surface-plasmon-enhanced optical forces in silver nanoaggregates," Phys. Rev. Lett., 89(24), 246802 (2002).
[10] F. Svedberg, Z. P. Li, H. X. Xu *et al.*, "Creating hot nanoparticle pairs for surface-enhanced Raman spectroscopy through optical manipulation," Nano Lett, 6(12), 2639-2641 (2006).
[11] Z. P. Li, M. Käll, and H. Xu, "Optical forces on interacting plasmonic nanoparticles in a focused Gaussian beam," Phy. Rev. B, 77(8), 085412 (2008).
[12] R. F. Oulton, V. J. Sorger, T. Zentgraf *et al.*, "Plasmon lasers at deep subwavelength scale," Nature, 461(7264), 629-632 (2009).
[13] P. Berini, and I. De Leon, "Surface plasmon-polariton amplifiers and lasers," Nature Photon., 6(1), 16-24 (2012).
[14] H. X. Xu, J. Aizpurua, M. Käll *et al.*, "Electromagnetic contributions to single-molecule sensitivity in surface-enhanced Raman scattering," Phys. Rev. E, 62(3), 4318-4324 (2000).
[15] H. X. Xu, and M. Käll, "Polarization-dependent surface-enhanced Raman spectroscopy of isolated silver nanoaggregates," Chemphyschem, 4(9), 1001-1005 (2003).
[16] H. Wei, U. Hakanson, Z. L. Yang *et al.*, "Individual nanometer hole-particle pairs for surface-enhanced Raman scattering," Small, 4(9), 1296-1300 (2008).
[17] H. Wei, F. Hao, Y. Z. Huang *et al.*, "Polarization dependence of surface-enhanced Raman scattering in gold nanoparticle-nanowire systems," Nano Lett, 8(8), 2497-2502 (2008).
[18] Y. R. Fang, H. Wei, F. Hao *et al.*, "Remote-Excitation Surface-Enhanced Raman Scattering Using Propagating Ag Nanowire Plasmons," Nano Lett, 9(5), 2049-2053 (2009).
[19] S. Mubeen, S. P. Zhang, N. Kim *et al.*, "Plasmonic Properties of Gold Nanoparticles Separated from a Gold Mirror by an Ultrathin Oxide," Nano Lett, 12(4), 2088-2094 (2012).
[20] L. Novotny, and N. van Hulst, "Antennas for light," Nature Photon., 5(2), 83-90 (2011).
[21] H. X. Xu, X. H. Wang, M. P. Persson *et al.*, "Unified treatment of fluorescence and Raman scattering processes near metal surfaces," Phys. Rev. Lett., 93(24), 243002 (2004).
[22] P. Johansson, H. X. Xu, and M. Käll, "Surface-enhanced Raman scattering and fluorescence near metal nanoparticles," Phys. Rev. B, 72(3), 035427 (2005).
[23] E. Prodan, C. Radloff, N. J. Halas *et al.*, "A hybridization model for the plasmon response of complex nanostructures," Science, 302(5644), 419-422 (2003).
[24] L. Mao, Z. P. Li, B. Wu *et al.*, "Effects of quantum tunneling in metal nanogap on surface-enhanced Raman scattering," Appl. Phys. Lett., 94(24), 243102 (2009).
[25] J. Zuloaga, E. Prodan, and P. Nordlander, "Quantum Description of the Plasmon Resonances of a Nanoparticle Dimer," Nano Lett, 9(2), 887-891 (2009).
[26] D. C. Marinica, A. K. Kazansky, P. Nordlander *et al.*, "Quantum Plasmonics: Nonlinear Effects in the Field Enhancement of a Plasmonic Nanoparticle Dimer," Nano Lett, 12(3), 1333-1339 (2012).
[27] R. Esteban, A. G. Borisov, P. Nordlander *et al.*, "Bridging quantum and classical plasmonics with a quantum-corrected model," Nat Commun, 3, 825 (2012).
[28] H. Ditlbacher, A. Hohenau, D. Wagner *et al.*, "Silver nanowires as surface plasmon resonators," Phys. Rev. Lett., 95(25), 257403 (2005).
[29] R. M. Dickson, and L. A. Lyon, "Unidirectional plasmon propagation in metallic nanowires," J. Phys. chem. B, 104(26), 6095-6098 (2000).

[30] H. Wei, D. Ratchford, X. Q. Li *et al.*, "Propagating Surface Plasmon Induced Photon Emission from Quantum Dots," Nano Lett*,* 9(12), 4168-4171 (2009).
[31] T. Shegai, V. D. Miljkovic, K. Bao *et al.*, "Unidirectional Broadband Light Emission from Supported Plasmonic Nanowires," Nano Lett*,* 11(2), 706-711 (2011).
[32] Z. P. Li, F. Hao, Y. Z. Huang *et al.*, "Directional Light Emission from Propagating Surface Plasmons of Silver Nanowires," Nano Lett*,* 9(12), 4383-4386 (2009).
[33] Z. P. Li, K. Bao, Y. R. Fang *et al.*, "Correlation between Incident and Emission Polarization in Nanowire Surface Plasmon Waveguides," Nano Lett*,* 10(5), 1831-1835 (2010).
[34] Z. P. Li, K. Bao, Y. R. Fang *et al.*, "Effect of a proximal substrate on plasmon propagation in silver nanowires," Phys. Rev. B*,* 82(24), 241402 (2010).
[35] W. H. Wang, Q. Yang, F. R. Fan *et al.*, "Light Propagation in Curved Silver Nanowire Plasmonic Waveguides," Nano Lett*,* 11(4), 1603-1608 (2011).
[36] S. P. Zhang, H. Wei, K. Bao *et al.*, "Chiral Surface Plasmon Polaritons on Metallic Nanowires," Phys. Rev. Lett*.,* 107(9), 096801 (2011).
[37] N. Liu, Z. Li, and H. Xu, "Polarization-Dependent Study on Propagating Surface Plasmons in Silver Nanowires Launched by a Near-Field Scanning Optical Fiber Tip," Small*,* doi: 10.1002/smll.201101809, (2012).
[38] Y. R. Fang, Z. P. Li, Y. Z. Huang *et al.*, "Branched Silver Nanowires as Controllable Plasmon Routers," Nano Lett*,* 10(5), 1950-1954 (2010).
[39] H. Wei, Z. P. Li, X. R. Tian *et al.*, "Quantum Dot-Based Local Field Imaging Reveals Plasmon-Based Interferometric Logic in Silver Nanowire Networks," Nano Lett*,* 11(2), 471-475 (2011).
[40] H. Wei, Z. X. Wang, X. R. Tian *et al.*, "Cascaded logic gates in nanophotonic plasmon networks," Nat Commun*,* 2, 387 (2011).
[41] Z. P. Li, S. P. Zhang, N. J. Halas *et al.*, "Coherent Modulation of Propagating Plasmons in Silver-Nanowire-Based Structures," Small*,* 7(5), 593-596 (2011).
[42] H. Wei, and H. Xu, "Nanowire-based plasmonic waveguides and devices for integrated nanophotonic circuits," Nanophotonics*,* doi: 10.1515/nanoph-2012-0012, (2012).